50th AIAA Aerospace Sciences Meeting including the New Horizons Forum and Aerospace Exposition
09 - 12 January 2012, Nashville, Tennessee

AIAA 2012-0410

Body Force Produced by a SDBD Plasma Actuator Using PIV Measurement

Jiapei Si[1,*], Borui Zheng[2,†], Sui Zheng[1,‡], Chao Gao[2,¶]
[1]*AVIC ChengDu Aircraft Design & Research Institute, Cheng du, 610041, China*

[2]*Northwestern Polytechnical University, Xi'an 710072, China*

Feng Liu[3,‖], and Shijun Luo[3,±]
[3]*University of California, Irvine, CA 92697-3975*

Downloaded by UNIVERSITY OF CALIFORNIA IRVINE on January 29, 2015 | http://arc.aiaa.org | DOI: 10.2514/6.2012-410

An experimental investigation on body force of Dielectric Barrier Discharge (DBD) plasma actuator aimed at low power flow control applications is presented. Momentum conservation equations have been adopted for a steady two dimensional laminar flow to calculate the body force produced by DBD plasma actuator. The momentum flux and viscous forces of different control volumes have been investigated, but the pressure force is neglected in the present work. Furthermore a parametric study on body force is conducted for a wide range of carrier frequency. It is shown that the body forces of different control volumes are different and for a given control volume the body force reaches a peak value when carrier frequency is at 25 kHz and the peak-peak voltage is at 12kV.

Nomenclature

abcda	=	control volume boundary
ds	=	element segment of abcda
F	=	force acting on abcda
F_B	=	body force induced by DBD actuation acting on abcda
F_p	=	pressure force acting on abcda
F_v	=	viscous force acting on abcda
f	=	ac source frequency
m	=	air mass
n	=	unit outward-normal of abcda
t	=	time
V	=	velocity
u	=	x-components of velocity V
v	=	y-components of velocity V
ρ	=	air density
μ	=	air viscosity

[*] Graduate Student, Department of General Design.
[†] Graduate Student, Department of Fluid Mechanics.
[‡] Researcher, General Office.
[¶] Professor and Vice Director, National Key Laboratory of Sceince and Technology on Aerodynamic Design and Research.
[‖] Professor, Department of Mechanical and Aerospace Engineering. Associate Fellow AIAA.
[±] Researcher, Department of Mechanical and Aerospace Engineering.

Copyright © 2012 by the authors. Published by the American Institute of Aeronautics and Astronautics, Inc., with permission.

Downloaded by UNIVERSITY OF CALIFORNIA IRVINE on January 29, 2015 | http://arc.aiaa.org | DOI: 10.2514/6.2012-410

I. Introduction

A dielectric barrier discharge, operating at kHz and kV conditions, can generate largely isothermal surface plasma and induce wall-jet like fluid flow. It can serve as an aerodynamic actuator, and has advantages of no moving parts. [1]

The resulting surface discharge generates momentum transfer to the ambient gas through collisions between energetic ions and neutral molecules in the ambient gas and induces ambient-gas motion along the surface. In order to better understand the mechanism of the momentum coupling between the plasma and the fluid flow, computational model of plasma is studied.

For most plasma flow-control cases, the time-scales ratios between those characterizing the discharge physics (convection, diffusion, and reaction/ionization) and the fluid flow mechanisms are separated by several decades, allowing the effect of plasma on the fluid dynamics modeled via a one-way body force treatment.

At a phenomenological level, Shyy et al. [2] had established the plasma models using linear force distribution to approximate the discharge structure. Enloe et al. [3] presented a high-fidelity approach using a first principle based hydrodynamic plasma models.

Direct measurements of the induced thrust were taken using a highly sensitive load cell by Abe et al.[4] A novel technique for determination of the spatial distribution of the body force was proposed, developed and tested by Kotsonis et al.[5], and they reported the use of a high-speed PIV system to resolve all terms of the Navier-Stokes equation representation of the flow field including body force. For steady flow, based on PIV measurements of the induced velocity field applying the momentum conservation equation on a control volume, the body force induced by the plasma jet was also calculated by assuming that the contributions of pressures and viscous forces over the control volume boundaries are neglected.

This paper investigates plasma induced body force over a flat plate in originally still air using the PIV cross-flow velocity measurements and the steady momentum conservation equation. The pressure contributions are neglected. However, deviating from momentum equations, the contributions of the viscous forces over the entire control volume boundary are studied. In the following sections, the experimental setup is presented. The convergence of the PIV data to a steady state is verified. The choice of the control volume size is studied and the contributions of the viscous normal and shear forces over the entire control volume boundaries to the plasma-induced body force of different a.c. source frequencies are investigated. Finally, conclusions are drawn.

II. Experimental Setup

A. Test model

Dielectric Barrier Discharge (DBD) actuators are used in the present research. The plasma actuator consists of two asymmetric copper electrodes each of 0.03 mm thickness. Five Kapton tape layers (0.04 mm thick per layer) separate the encapsulated electrode from the exposed electrode. The effective spanwise length (along which plasma is generated) is 150 mm. The width of the exposed and encapsulated electrode is 1 mm and 2 mm, respectively. The two electrodes are separated by a gap, which is 1.5 mm in all test cases. A plexiglas plate of 300 mm wide and 400mm long and 5mm thick is utilized as the support of the actuator which is glued to the central area of the plexiglas plate.

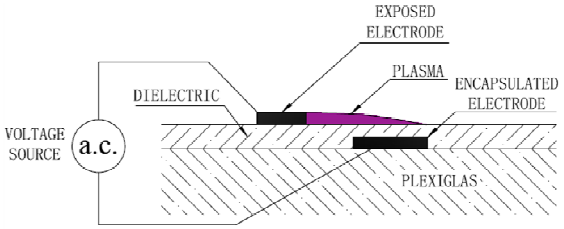

Figure 1. The geometrical properties of the plasma actuator

To reduce the effect of any external disturbances on the measurement, all tests are conducted in still air which is achieved by a closed cuboid chamber with a length of 600 mm, a width of 500 mm and a height of 500 mm. The bottom is the surface of a test table, and the other five faces of the chamber are made from plexiglas of 5 mm thick to allow for optical viewing and access of the laser sheet. The air inside the chamber under one atmospheric pressure

is shielded from the air in the laboratory room. The seeds are smoke particles of approximately 1 μm in diameter commonly used in cinema industry. The seeds would stay suspended for many hours and were only replenished when needed.

The actuator is driven by the same multi-channel plasma generator as in Ref. 6. The waveform of the a.c. source is sine wave. The peak-to-peak voltage is set at V_{p-p} = 12 kV and carrier frequency changes from 10 kHz to 50 kHz. The output voltage is measured by a high voltage probe, while the current is read on the plasma generator. All the tests in this paper are continuous discharge actuation.

B. PIV Setup

The PIV system is manufactured by the Dantec Dynamic Company. The Nd:YAG Laser, a product of the Beamtech Optronics Co., emits single pulse of energy ≤ 200 mJ and produces double pulses with a time interval of 60 μs. The laser sheet is in 1 mm thickness. The repeat rate of the laser double-pulse is set at 15 Hz. Consecutive 15 seconds of sampling are performed for each case. The sampling number for ensemble averages is 225. A CCD camera of 1600 × 1200 pixels is used to capture the field-of-view of 36 mm × 25 mm. A software of DynamicStudio 2.30.47 version is used to calculate the cross-flow velocity vector field from the double-pulse images. Table 1 shows the input power is approximately proportional to the carrier frequency.

Table 1. Input power versus carrier frequency, V_{p-p}= 12 kV

Frequency (kHz)	**10**	**15**	**20**	**25**	**30**	**35**	**40**	**45**	**50**
Voltage (V)	120	120	120	120	120	120	120	120	120
Current (A)	0.3	0.5	0.65	0.8	1	1.25	1.5	1.6	1.7
Input power (W)	36	60	78	96	120	150	180	192	204

The momentum equations in steady form are used thus the flow field must keep steady state during PIV data acquisition. It takes approximately 5 seconds to start power supple and stabilize the output voltage and nearly 10 seconds are needed to make the flow become steady. So in order to obtain a steady flow field, the plasma actuator has to work for 15 seconds before PIV acquisition starts. It should be noted that no other filtering or smoothing has been applied apart from the processing of the raw PIV data and time averaging.

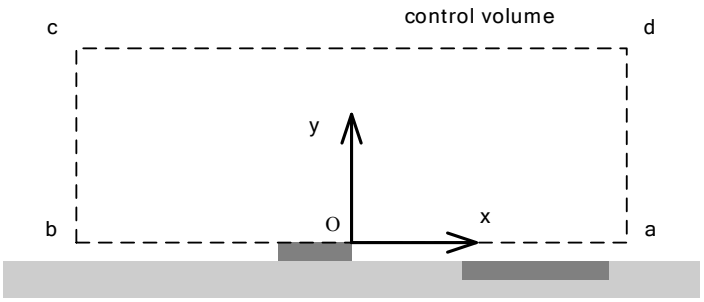

Figure 2. The control volume for the momentum balance equations

The origin of the coordinate system is located at the downstream upper edge of the exposed electrode as shown in Fig. 2. Two points, one is upstream of the actuator and the other is downstream, are chosen arbitrarily to check the steady flow. The component velocity of different sampling time has been analyzed in Fig. 3. The results show that the flow has been steady already. Fig. 3 (b) shows the u velocity fluctuates dramatically and vibrates around u = 0.5m/s, this may be caused by the irregular fluctuation of carrier frequency.

Downloaded by UNIVERSITY OF CALIFORNIA IRVINE on January 29, 2015 | http://arc.aiaa.org | DOI: 10.2514/6.2012-410

Downloaded by UNIVERSITY OF CALIFORNIA IRVINE on January 29, 2015 | http://arc.aiaa.org | DOI: 10.2514/6.2012-410

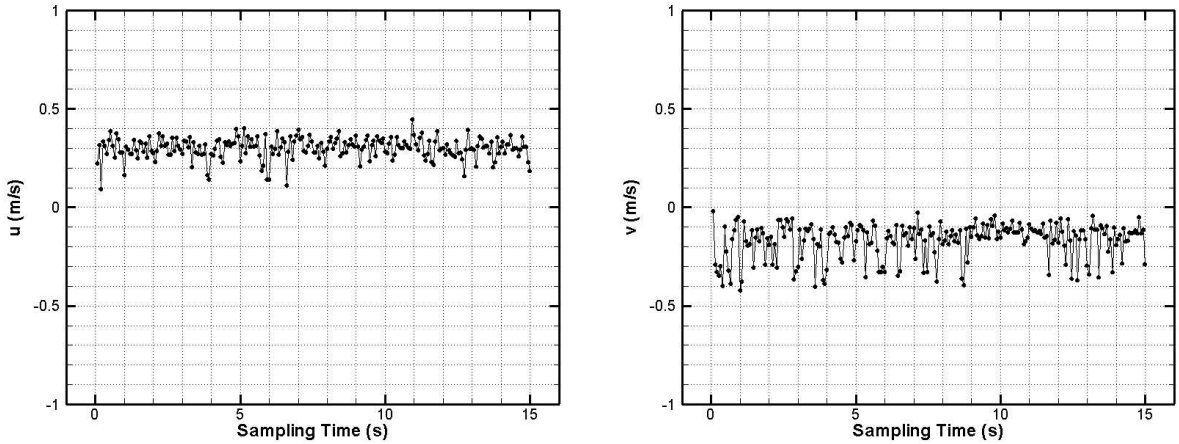

(a) x = 3 mm, y = 1.88 mm

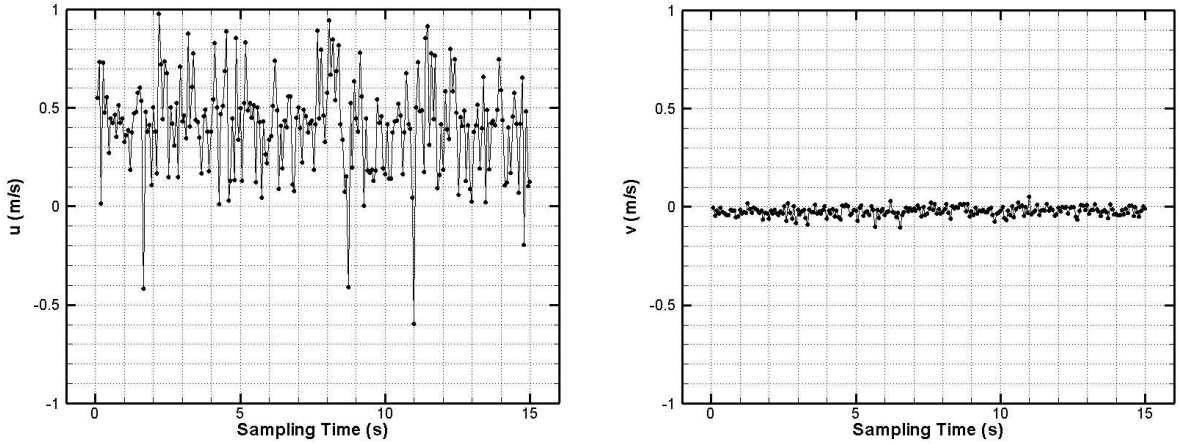

(b) x = -3 mm, y = 1.12 mm

Figure 3. Time evolution of velocity

The case of f = 15 kHz has been selected to study the convergence of ensemble-averaged cross-flow velocity versus sampling time. On the cross-flow plane, a fixed point of x = 21.02 cm and y = 0.28 cm is selected, where the ensemble-averaged maximum cross-flow velocity obtained from the PIV sampling time of 15 s in the entire neighborhood of the plate surface is located. At this point, the ensemble-averaged cross-flow velocities over sampling time of 1, 5, 10 and 15 seconds are listed in Tab. 2. It can be concluded the sampling time of 15 seconds yields convergent result.

Table 2. Convergence of ensemble-averaged cross-flow velocity versus sampling time

PIV sampling time (s)	1	5	10	15
Cross-flow velocity (m/s)	2.198	2.213	2.240	2.234

III. Momentum Equations

The body force induced by plasma actuation can be calculated via momentum equation of the induced flow field. A control volume is taken by which the body force is calculated from the equilibrium of the momentum flux and the exerted forces (Fig. 2). Because the actuator spans 150mm in length and has a width of 4.5mm (induced

main flow direction), so the flow is supposed to be steady two-dimensional except near the two ends.

Newton's second law can be written as

$$\vec{F} = \frac{d(m\vec{V})}{dt} \tag{1}$$

The left side of equation Eq. (1) is

$$F = F_B + F_v + F_p \tag{2}$$

which is the force exerted on the fluid as it flows through the control volume.

Because the flow is steady and two dimensional, so the right side of Eq. (1) is

$$\frac{d(m\vec{V})}{dt} = \oint_{abcda} (\rho\vec{V} \cdot \vec{n}ds)\vec{V} \tag{3}$$

which is the time rate of change of momentum of the fluid as it sweeps through the fixed control volume.

Combining Eq. (2) and (3), we obtain the momentum in integral form.

$$\oint_{abcda} (\rho\vec{V} \cdot \vec{n}ds)\vec{V} = F_B + F_v + F_p \tag{4}$$

and the body force on the control volume is therefore

$$F_B = \oint_{abcda} (\rho\vec{V} \cdot \vec{n}ds)\vec{V} - F_v - F_p \tag{5}$$

where F_B is body force exerted on the fluid, F_v is viscous force, F_p is pressure force. Because the flow velocity is very slow in the present study, so the flow is considered to be incompressible and the air density ρ is constant.

The flow is assumed laminar, and the momentum flux, viscous force and pressure force can be written as

x - direction

$$\oint_{abcda} (\rho\vec{V} \cdot \vec{n}ds)u = \rho\int_{da} u^2 dy + \rho\int_{cd} uvdx - \rho\int_{bc} u^2 dy \tag{6}$$

$$F_{v,x} = \int_{cd} \mu(\frac{\partial v}{\partial x} + \frac{\partial u}{\partial y})dx - \int_{ab} \mu(\frac{\partial v}{\partial x} + \frac{\partial u}{\partial y})dx - \int_{bc} 2\mu\frac{\partial u}{\partial x}dy + \int_{ad} 2\mu\frac{\partial u}{\partial x}dy \tag{7}$$

$$F_{p,x} = \int_{bc} pdy - \int_{ad} pdy \tag{8}$$

y - direction

$$\oint_{abcda} (\rho\vec{V} \cdot \vec{n}ds)v = \rho\int_{da} uvdy + \rho\int_{cd} v^2 dx - \rho\int_{bc} uvdy \tag{9}$$

$$F_{v,y} = \int_{ad} \mu(\frac{\partial v}{\partial x} + \frac{\partial u}{\partial y})dy - \int_{bc} \mu(\frac{\partial v}{\partial x} + \frac{\partial u}{\partial y})dy - \int_{ba} 2\mu\frac{\partial v}{\partial y}dx + \int_{cd} 2\mu\frac{\partial v}{\partial y}dx \tag{10}$$

$$F_{p,y} = \int_{ab} pdy - \int_{cd} pdy \tag{11}$$

Substituting Eqs. (6), (7) and (8) into Eq. (5) yields the body force in x-direction

$$\begin{aligned} F_{B,x} &= \oint_{abcda} (\rho\vec{V} \cdot \vec{n}ds)u - F_{v,x} - F_{p,x} \\ &= \rho\int_{da} u^2 dy + \rho\int_{cd} uvdx - \rho\int_{bc} u^2 dy \\ &- [\int_{cd} \mu(\frac{\partial v}{\partial x} + \frac{\partial u}{\partial y})dx - \int_{ab} \mu(\frac{\partial v}{\partial x} + \frac{\partial u}{\partial y})dx - \int_{bc} 2\mu\frac{\partial u}{\partial x}dy + \int_{ad} 2\mu\frac{\partial u}{\partial x}dy] - (\int_{bc} pdy - \int_{ad} pdy) \end{aligned} \tag{12}$$

Substituting Eqs. (9), (10) and (11) into Eq. (5) yields the body force in y-direction

Downloaded by UNIVERSITY OF CALIFORNIA IRVINE on January 29, 2015 | http://arc.aiaa.org | DOI: 10.2514/6.2012-410

$$F_{B,y} = \oint_{abcda} (\rho \vec{V} \cdot \vec{n} ds) v - F_{v,y} - F_{p,y}$$

$$= \rho \int_{da} uvdy + \rho \int_{cd} v^2 dx - \rho \int_{bc} uvdy \tag{13}$$

$$-[\int_{ad} \mu(\frac{\partial v}{\partial x} + \frac{\partial u}{\partial y})dy - \int_{bc} \mu(\frac{\partial v}{\partial x} + \frac{\partial u}{\partial y})dy - \int_{ba} 2\mu \frac{\partial v}{\partial y} dx + \int_{cd} 2\mu \frac{\partial v}{\partial y} dx] - (\int_{ab} pdy - \int_{cd} pdy)$$

Equations (12) and (13) are formulas of body force induced by plasma. In the formulas the partial differential derivatives must be calculated first, and the central and one-sided finite-differences, which are second order accuracy finite differences, can be used to calculate them.

Central finite difference of second order of accuracy is

$$\frac{\partial f}{\partial x} = [f(x+h) - f(x-h)]/(2h) + O(h^2) \tag{14}$$

One-side finite difference of second order of accuracy is

$$\frac{\partial f}{\partial x} = [-f(x+2h) + 4f(x+h) - 3f(x)]/(2h) + O(h^2) \tag{15}$$

where h is a constant step of the finite difference.

The approximation of the derivatives with respect to *x* coordinate only needs central difference, whereas for the approximation of the derivatives with respect to *y*, one-sided finite-difference is needed at the bottom of the computational domain along *y*-direction (i.e., the bottom of the chamber), and central difference is used in the rest region.

IV. Calculation of Plasma-Induced Body Force

The time averaged flow field with the selected control volume I is given in Fig. 4. The exposed electrode is located between x = -1 mm and x = 0 mm and the encapsulated electrode is located between x = 1.5 mm and x = 3.5mm. The dark arrows stand for the velocity vector and the contour between different colors represents the ensemble-averaged crossflow-velocity isoline.

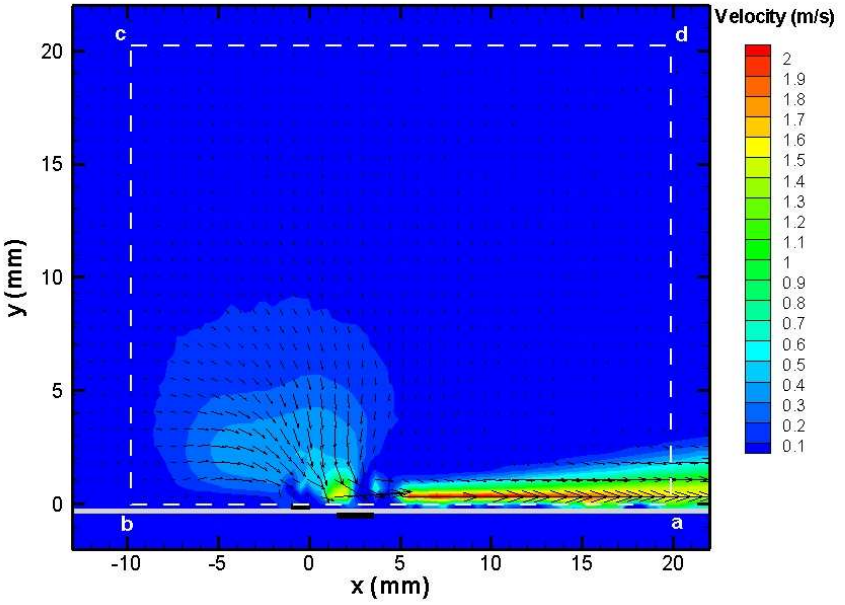

Figure 4. Time averaged total velocity field and control volume for momentum balance (12 kV_{p-p}, 15 kHz)

Downloaded by UNIVERSITY OF CALIFORNIA IRVINE on January 29, 2015 | http://arc.aiaa.org | DOI: 10.2514/6.2012-410

Four sets of control volume have been selected to calculate the body force and viscous force. And the position of control volumes has been listed in Tab. 3. It can be concluded that the x-direction body force decreases and y-direction body force increases as the control volume becomes small, but the viscous force has little change both in x- and y-directions. This may be caused by less momentum flux flowing though the control volume.

Table 3. The position of the four control volumes

	I	II	III	IV
a	(19.90,0)	(10.13,0)	(4.88,0)	(3.38,0)
b	(-9.76,0)	(-4.88 ,0)	(-4.88,0)	(-1.13,0)
c	(-9.76, 20.27)	(-4.88,10.13)	(-4.88, 4.88)	(-1.13, 1.87)
d	(19.90, 20.27)	(10.13,10.13)	(4.88, 4.88)	(3.38, 1.87)

Table 4. Body force of each boundary of the control volume I

	Momentum Flux (mN/m)				Viscous Force (mN/m)					F_B (mN/m)
	bc	cd	da	subtotal	ab	bc	cd	da	subtotal	
x	-0.106	-2.82E-02	3.257	3.124	-2.142	-2.97E-03	-1.09E-04	2.95E-04	-2.144	5.268
y	3.65E-02	3.86E-02	-2.00E-03	0.073	0.103	1.10E-04	2.54E-03	-9.19E-03	0.097	-0.024

Table 5. Body force of each boundary of the control volume II

	Momentum Flux (mN/m)				Viscous Force (mN/m)					F_B (mN/m)
	bc	cd	da	subtotal	ab	bc	cd	da	subtotal	
x	-0.484	-3.65E-02	2.143	1.622	-1.143	5.95E-05	7.62E-04	6.32E-03	-1.135	2.758
y	0.142	7.65E-02	2.48E-03	0.221	8.46E-02	3.98E-03	3.31E-03	-2.75E-03	0.089	0.132

Table 6. Body force of each boundary of the control volume III

	Momentum Flux (mN/m)				Viscous Force (mN/m)					F_B (mN/m)
	bc	cd	da	subtotal	ab	bc	cd	da	subtotal	
x	-0.427	-0.140	1.848	1.281	-0.287	-8.88E-04	-2.71E-03	1.05E-02	-0.281	1.562
y	9.97E-02	0.439	5.74E-03	0.545	4.40E-02	9.26E-04	1.75E-02	-2.57E-03	0.060	0.485

Table 7. Body force of each boundary of the control volume IV

	Momentum Flux (mN/m)				Viscous Force (mN/m)					F_B (mN/m)
	bc	cd	da	subtotal	ab	bc	cd	da	subtotal	
x	-0.238	-0.307	5.25E-02	-0.492	-0.167	-7.52E-03	-1.87E-02	-2.26E-02	-0.216	-0.276
y	8.23E-02	0.561	-2.57E-03	0.641	2.32E-02	-5.00E-04	-1.36E-02	-1.00E-03	8.12E-03	0.632

Downloaded by UNIVERSITY OF CALIFORNIA IRVINE on January 29, 2015 | http://arc.aiaa.org | DOI: 10.2514/6.2012-410

V. Effects of Carrier Frequency on Body Force

The momentum flux, viscous force and body force of different carrier frequencies have been listed in Tab. 8. The control volume I is employed here. The viscous force over the control volume is generally not negligible. The pressure force is ignored due to lack of the information of pressure from the PIV velocity data. The effects of the a.c. source frequency from 10 to 50 kHz with peak-to-peak voltage of 12 kV on the body force are studied.

Table 8. Section contribution in thrust (mN/m) for 10 kHz - 50 kHz, 12 kV_{p-p}

f	Momentum Flux		Viscous Force		Body Force	
	x	***y***	***x***	***y***	***x***	***y***
10kHz	3.084	0.081	-0.803	0.073	3.887	0.008
15kHz	3.124	0.073	-2.144	0.097	5.268	-0.024
20kHz	3.946	0.085	-2.446	4.63E-03	6.392	0.081
25kHz	6.939	0.344	-2.600	0.339	9.538	0.004
30kHz	6.517	0.422	-1.263	0.219	7.780	0.203
35kHz	3.004	0.405	-0.894	0.233	3.898	0.171
40kHz	4.496	0.374	-0.803	-0.344	5.300	0.719
45kHz	1.908	0.312	-0.262	0.292	2.170	0.020
50kHz	2.730	0.151	-0.029	-0.167	2.759	0.318

Figure 5 illustrates the body forces of x-/y-direction at various carrier frequencies. It can be concluded the body force in x-direction is less than 10 mN/m, while the body force in y-direction remains constant. Surprisingly, the x-direction body force reaches a peak value of 9.546 mN/m at f = 25 kHz under the input power of 96W, which gives a body force per unit power of approximate 0.1 mN/W. This value is close to that of the thrust force of 0.2mN/W measured by Gregory et al.[7], and the difference between the two results might be attributed to the ignorance of pressure force in the computations in this paper. The frequency of 25 kHz might be regarded as an optimal frequency to provide the best actuation and thus can be utilized to promote the effectiveness of flow control although the reason for this is still unclear.

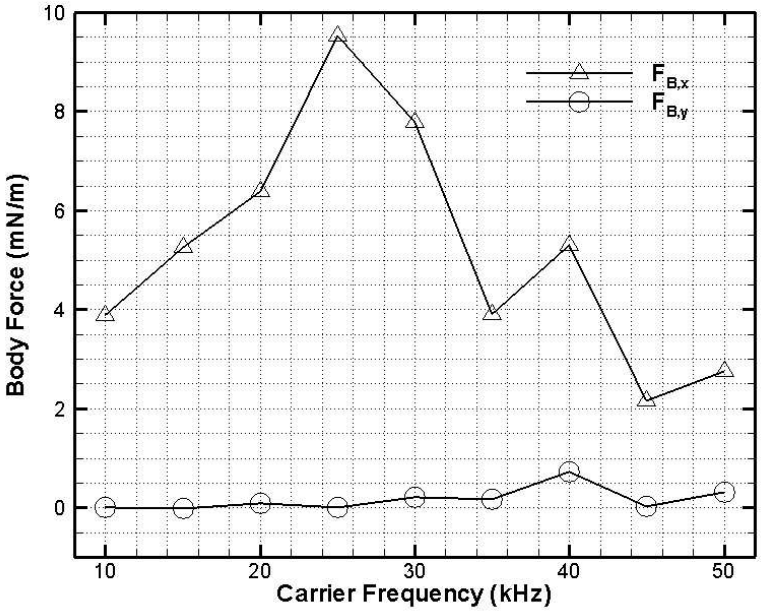

Figure 5. Body force for carrier frequency changing from 10 kHz - 50 kHz, 12 kV_{p-p}

Downloaded by UNIVERSITY OF CALIFORNIA IRVINE on January 29, 2015 | http://arc.aiaa.org | DOI: 10.2514/6.2012-410

VI. Conclusions

A two-dimensional steady flow is generated by a slender dielectric barrier discharge plasma actuator actuated with a constant a.c. voltage source in an originally still air under one atmosphere pressure. The flow field is measured by a particle image velocimetry (PIV). The resultant body force induced by the plasma actuation over the ambient air is estimated using the momentum equation over a control volume. The momentum flux and the viscous force in the momentum equation are calculated from the PIV measurement. However, the pressure force is unavailable and ignored in the present paper.

Body forces for four different control volumes under the same a.c. voltage source are compared. The effects of the a.c. source frequency from 10 to 50 kHz with peak-to-peak voltage of 12 kV on the body force are studied. The ignorance of the pressure force over the control volume is in doubt and its measurement is being carried out by the present authors.

Downloaded by UNIVERSITY OF CALIFORNIA IRVINE on January 29, 2015 | http://arc.aiaa.org | DOI: 10.2514/6.2012-410

Acknowledgments

The present work is supported by the Specialized Research Fund for Doctoral Program of Higher Education, SPFDP-200806990003, and the Foundation for Fundamental Research of the Northwestern Polytechnical University, NPU-FFR-W018102 and JC201103. The authors would like to thank Ya Liu of University of California, Irvine and Yushuai Wang of Northwestern Polytechnical University for their technical assistance.

References

[1] Roth, J. R., Sherman, D. M., and Wilkinson, S. P., "Boundary Layer Flow Control with a One Atmosphere Uniform Glow Discharge Surface Plasma," *AIAA Paper*, 1998-0328, Aerospace Sciences Meeting and Exhibit, 36th, Reno, NV, Jan. 12-15, 1998.

[2] Shyy, W., Jayaraman, B., and Anderson, A., "Modeling of Glow-Discharge Induced Flow Dynamics," *Journal of Applied Physics*, Vol. 92, No. 11, 2002, pp. 6434–43.

[3] Enloe, C.L., Mclaughlin, T.E., Van Dyken, R.D., Kachner, K.D., Jumper, E.J., and Corke, T.C. "Mechanisms and Responses of a Single Dielectric Barrier Plasma Actuator: Geometric Effects," *AIAA Journal*, Vol. 42, No. 3, 2004, pp. 595–604.

[4] Abe, T., Takizawa, Y., Sato, S., and Kimura, N., "Experimental Study for Momentum Transfer in a Dielectric Barrier Discharge Plasma Actuator," *AIAA Journal*, Vol.46, No.9, 2008, pp.2248-2256.

[5] Kotsonis, M., Ghaemi, S., Giepman, R., and Veldhuis, L., "Experimental Study on the Body Force Field of Dielectric Barrier Discharge Actuators" , *AIAA Paper*, 2010-4630, 41st Plasma dynamics and Lasers Conference, Chicago, Illinois, Jun., 2010.

[6] Zheng, B.R., Gao, C., Li, Y.B., Liu, F., and Luo, S.J., "Momentum Transfer in Millisecond Periodic-Pulsed Dielectric-Barrier-Discharge Plasma Actuator" , *AIAA Paper*, 2011-739, 49th AIAA Aerospace Sciences Meeting including the New Horizons Forum and Aerospace Exposition, Orlando, Florida, Jan., 2011.

[7] Gregory, J. W., Enloe, C. L., Font, G. I., and McLaughlin, T. E., "Force Production Mechanisms of a Dielectric-Barrier Discharge Plasma Actuator," *AIAA Paper*, 2007-185, Jan., 2007.